On the prompt contribution to the atmospheric neutrino flux

Sergey Ostapchenko, Maria Vittoria Garzelli, and Günter Sigl
Universität Hamburg, II Institut für Theoretische Physik, 22761 Hamburg, Germany

(Received 1 September 2022; accepted 19 December 2022; published 19 January 2023)

The prompt contribution to the atmospheric neutrino flux is analyzed. We demonstrate that the corresponding theoretical uncertainties related to perturbative treatment of charm production, notably, the ones stemming from the low- and high-x behavior of parton distribution functions, can be conveniently studied at the level of charm quark production. Additionally, we discuss the nonperturbative contribution to the prompt neutrino flux, related to the intrinsic charm content of the proton and analyze its main features.

DOI: 10.1103/PhysRevD.107.023014

I. INTRODUCTION

The detection of astrophysical neutrino fluxes by the IceCube experiment [1,2] paves the way for establishing neutrino astronomy as a viable method for studying the remote Universe. Among the relevant research activities are ones aiming at a reliable estimation of the background for such measurements, produced by cosmic ray (CR) interactions in the atmosphere of Earth [3–6]. Particular attention is paid to calculations of the so-called prompt neutrino flux resulting from decays of charmed hadrons produced in such interactions, which dominates the atmospheric neutrino background for neutrino energies $E_\nu \gtrsim 1$ PeV [7–9].

A number of analyses have been devoted to studies of prompt neutrino production, comparing different approaches to the problem, investigating the impact of present uncertainties regarding parton distribution functions (PDFs) of protons and nuclei, and studying the dependence of the results on the employed parametrizations of the primary CR fluxes [10–14].

In this work, we choose to address the problem at the level of the production cross sections for charm (anti) quarks, using the collinear factorization framework of the perturbative quantum chromodynamics (pQCD). We demonstrate that the relevant fragmentation functions for charm (anti)quarks, as well as the decay distributions for charmed hadrons, can be factorized out, such that the relevant input from pQCD is described by CR spectrum-weighted moments ("Z factors") of production spectra for charm (anti)quarks. This proves to be convenient for studying the relevant uncertainties, notably, regarding the PDFs involved, and for specifying the kinematic regions relevant for such calculations.

Additionally, we discuss the nonperturbative contribution to the prompt neutrino flux, related to the intrinsic charm content of the proton and demonstrate that the corresponding Z factors take a particularly simple form. However, our approach may be inapplicable to the case of nonperturbative charm production because of potentially different hadronization mechanisms in such a case.

The outline of the paper is as follows. In Sec. II, we present our formalism and derive a relation between the perturbative contribution to the prompt atmospheric neutrino flux and the respective Z factor for charm production. In Sec. III, we present the corresponding numerical results and analyze their dependence on the gluon PDFs in use. Section IV is devoted to a discussion of the intrinsic charm contribution. Finally, we conclude in Sec. V.

II. FORMALISM

The main contribution to prompt atmospheric neutrinos is generated by the proton component of the primary CR flux. Concentrating, for definiteness, on the muonic (anti)neutrinos, the relevant range of neutrino energies extends from few hundred TeV to ∼10 PeV, since for higher neutrino energies interactions of their would-be parent charmed hadrons start to prevail over their decays. In turn, this involves interactions of primary protons at energies above the so-called "knee" of the CR spectrum at $E_{\rm knee} \simeq 3$–4 PeV [15] and below the proton "ankle" at $E \simeq 100$ PeV [16]. In that energy range, the CR proton spectrum can be approximated by a power law behavior,

$$I_p(E_0) \simeq I_p(E_{\rm knee})(E_0/E_{\rm knee})^{-\gamma_p}, \tag{1}$$

with $\gamma_p \simeq 3.1$–3.3 [16–20].

For the corresponding prompt neutrino flux, one obtains [3,4,7]

$$I^{(p)}_{\nu_\mu(\mathrm{prompt})}(E_\nu) \simeq \int dE_0 \frac{I_p(E_0)}{1 - Z^p_{p\text{-air}}(E_0)} \times \frac{dn^{\nu_\mu(\mathrm{prompt})}_{p\text{-air}}(E_0, E_\nu)}{dE_\nu}, \quad (2)$$

where $dn^{\nu_\mu(\mathrm{prompt})}_{p\text{-air}}/dE_\nu$ is the inclusive spectrum of muon (anti)neutrinos resulting from decays of charmed hadrons produced in p-air interactions, and $Z^p_{p\text{-air}}$ is the spectrum-weighted moment for proton "regeneration,"

$$Z^p_{p\text{-air}}(E) = \int dE_0 \frac{I_p(E_0)}{I_p(E)} \frac{dn^p_{p\text{-air}}(E_0, E)}{dE}, \quad (3)$$

with $dn^p_{p\text{-air}}/dE$ being the energy distribution of secondary protons in proton-air collisions.

For the power law primary flux (1), Eq. (2) can be transformed to

$$I^{(p)}_{\nu_\mu(\mathrm{prompt})}(E_\nu) \simeq I_p(E_{\mathrm{knee}}) \frac{(E_\nu/E_{\mathrm{knee}})^{-\gamma_p}}{1 - Z^p_{p\text{-air}}(E_\nu, \gamma_p)} \times Z^{\nu_\mu(\mathrm{prompt})}_{p\text{-air}}(E_\nu, \gamma_p), \quad (4)$$

where we used the weak energy dependence of the factor $(1 - Z^p_{p\text{-air}})^{-1}$ [7] to take it out of the integral, while the spectrum-weighted moments (Z factors) $Z^X_{p\text{-air}}$, $X = p, \nu_\mu$ (prompt), are now defined as

$$Z^X_{p\text{-air}}(E, \gamma_p) = \int dx\, x^{\gamma_p - 1} \frac{dn^X_{p\text{-air}}(E/x, x)}{dx}. \quad (5)$$

Here $dn^X_{p\text{-air}}/dx$ is the distribution of the produced particles X, with respect to the energy fraction $x = E_X/E_0$ taken from the parent proton. For the prompt neutrino production, it is expressed via convolutions of the respective distributions of charmed hadrons $dn^{h_c}_{p\text{-air}}/dx_h$, with the corresponding decay distributions $f^{\mathrm{dec}}_{h_c \to \nu_\mu}$ summed over the hadron species,

$$\frac{dn^{\nu_\mu(\mathrm{prompt})}_{p\text{-air}}(E, x_\nu)}{dx_\nu} = \sum_{h_c} \int_{x_\nu}^1 \frac{dx_h}{x_h} \times \frac{dn^{h_c}_{p\text{-air}}(E, x_h)}{dx_h} f^{\mathrm{dec}}_{h_c \to \nu_\mu}(x_\nu/x_h). \quad (6)$$

In the high-energy limit we are interested in, one can neglect the dependence of $f^{\mathrm{dec}}_{h \to \nu_\mu}$ on the hadron energy, while the neutrino energy fraction x_ν/x_h is indistinguishable from the respective light-cone plus (LC^+) momentum fraction $(E_\nu + p_{z_\nu})/(E_h + p_{z_h})$ [21].

In the collinear factorization framework, $dn^{h_c}_{p\text{-air}}/dx_h$ can be expressed via the inclusive cross section for charm (anti) quark production $d\sigma^{c(\bar{c})}_{p\text{-air}}/dx_c$ as follows:

$$\frac{dn^{h_c}_{p\text{-air}}(E, x_h)}{dx_h} = \frac{1}{\sigma^{\mathrm{inel}}_{p\text{-air}}(E)} \sum_{c,\bar{c}} \int_{x_h}^1 \frac{dx_c}{x_c} \times \frac{d\sigma^{c(\bar{c})}_{p\text{-air}}(E, x_c)}{dx_c} D_{c(\bar{c}) \to h_c}(x_h/x_c). \quad (7)$$

Here we neglected the dependence of the charm (anti)quark fragmentation functions $D_{c(\bar{c}) \to h_c}$ on the factorization scale for hard parton scattering; $\sigma^{\mathrm{inel}}_{p\text{-air}}$ is the inelastic proton-air cross section.

Making use of Eq. (7) in Eq. (6), inserting the result into Eq. (5), and changing to integration variables $z_\nu = x_\nu/x_c$, $z_h = x_h/x_c$, we obtain

$$Z^{\nu_\mu(\mathrm{prompt})}_{p\text{-air}}(E_\nu, \gamma_p) = \int_0^1 dz_\nu H(z_\nu, \gamma_p) \times Z^c_{p\text{-air}}(E_\nu/z_\nu, \gamma_p). \quad (8)$$

Here $Z^c_{p\text{-air}}$ is defined by Eq. (5), for $X = c$, and

$$H(z_\nu, \gamma_p) = z_\nu^{\gamma_p - 1} \sum_{c,\bar{c}} \sum_{h_c} \int_{z_\nu}^1 \frac{dz_h}{z_h} \times D_{c(\bar{c}) \to h_c}(z_h) f^{\mathrm{dec}}_{h_c \to \nu_\mu}(z_\nu/z_h). \quad (9)$$

Finally, noting that small values of z_ν in the integrand on the right-hand side (rhs) of Eq. (8) are suppressed by the factor $z_\nu^{\gamma_p - 1}$ [cf. Eq. (9)] and assuming that $Z^c_{p\text{-air}}(E_\nu/z_\nu, \gamma_p)$ changes weakly in the relevant range of z_ν, we get

$$Z^{\nu_\mu(\mathrm{prompt})}_{p\text{-air}}(E_\nu, \gamma_p) \simeq Z^c_{p\text{-air}}(E_\nu, \gamma_p) \times \left[\sum_{c,\bar{c}} \sum_{h_c} Z^{\mathrm{fragm}}_{c(\bar{c}) \to h_c}(\gamma_p) Z^{\mathrm{dec}}_{h_c \to \nu_\mu}(\gamma_p) \right], \quad (10)$$

with

$$Z^{\mathrm{fragm}}_{c(\bar{c}) \to h_c}(\gamma_p) = \int_0^1 dz\, z^{\gamma_p - 1} D_{c(\bar{c}) \to h_c}(z), \quad (11)$$

$$Z^{\mathrm{dec}}_{h_c \to \nu_\mu}(\gamma_p) = \int_0^1 dz\, z^{\gamma_p - 1} f^{\mathrm{dec}}_{h_c \to \nu_\mu}(z). \quad (12)$$

We can see that all the pQCD input in Eqs. (8) and (10) are contained in the CR spectrum-weighted moments $Z^c_{p\text{-air}}$

of the energy distributions of charm quarks produced in proton-air interactions, which allows one to study the respective uncertainties at the level of c-quark production.

Let us now briefly comment on the contributions of primary nuclear species to the prompt atmospheric neutrino flux. While partial spectra for various nuclear mass groups of the primary CRs are not well determined at the energies of our interest, there are strong experimental indications that those contain spectral breaks (knees) at energies Z_i times higher than the one of the proton knee, Z_i being the characteristic charge for the ith group, and the respective spectral slopes γ_i above the breaks are not too different from the proton slope γ_p [16–20,22,23]. To some extent, this is indeed expected, if all the primary species come from the same kind of astrophysical sources. Adopting such a picture, partial fluxes of various nuclear mass groups of the primary CRs can also be described by the corresponding power laws,

$$I_{A_i}(E_0) \simeq I_{A_i}(Z_i E_{\rm knee}) \left(\frac{E_0}{Z_i E_{\rm knee}}\right)^{-\gamma_i}, \tag{13}$$

E_0 being here the energy per nucleus. Further, since the prompt neutrino yield is intimately related to forward (high x_c) charm (anti)quark production, the so-called superposition model (see, e.g., Ref. [24]) is fully applicable here: the neutrino yield from a primary nucleus of mass number A_i and energy E_0 can be approximated by A_i times the yield from a primary proton of energy E_0/A_i. This leads us to [cf. Eq. (4)]

$$I^{(A_i)}_{\nu_\mu({\rm prompt})}(E_\nu) \simeq \frac{A_i^{2-\gamma_i} I_{A_i}(Z_i E_{\rm knee})}{1 - Z^p_{p\text{-air}}(E_\nu, \gamma_i)} \times \left(\frac{E_\nu}{Z_i E_{\rm knee}}\right)^{-\gamma_i} Z^{\nu_\mu({\rm prompt})}_{p\text{-air}}(E_\nu, \gamma_i). \tag{14}$$

Thus, also in that case, the problem is reduced to a calculation of the CR spectrum-weighted moments $Z^{\nu_\mu({\rm prompt})}_{p\text{-air}}$—this time, using the corresponding slope γ_i for a primary nuclear mass group of interest. Second, let us recall that the relative abundances of the main primary mass groups are of the same order of magnitude at the proton knee energy (see, e.g., Refs. [17,20]). Therefore, if the primary spectral slopes for these groups are indeed similar to the one for primary protons, $\gamma_i \simeq \gamma_p$, Eq. (14) tells us that significant contributions to the prompt atmospheric neutrino flux come from CR protons and helium nuclei only, with the summary contribution of heavier primaries being a $\sim$10% correction.

III. NUMERICAL RESULTS

As the dominant contribution to charm (anti)quark production comes from the gluon-gluon fusion process (see, e.g., [25]) and the gluon PDF of a nucleus can be approximated by a superposition of the ones of its nucleons,[1] we have

$$Z^c_{p\text{-air}}(E,\gamma) \simeq \int dx_c x_c^{\gamma-1} \frac{\langle A_{\rm air}\rangle}{\sigma^{\rm inel}_{p\text{-air}}(E/x_c)} \frac{d\sigma^{c(gg)}_{pp}(E/x_c, x_c)}{dx_c}, \tag{15}$$

where $\langle A_{\rm air}\rangle$ is the average mass number for air nuclei[2] and $d\sigma^{c(gg)}_{pp}/dx_c$ is defined by the usual collinear factorization ansatz as follows:

$$\frac{d\sigma^{c(gg)}_{pp}(E_p, x_c)}{dx_c} = \int dx^+ dx^- \int d^2k_{\perp_c} dy^*_c \times \frac{d^3\hat\sigma_{gg\to c}(\hat s, y^*_c, k_{\perp_c}, \mu_{\rm F}, \mu_{\rm R})}{dy^*_c dk^2_{\perp_c}} g_p(x^+, \mu_{\rm F}) \times g_p(x^-, \mu_{\rm F})\, \delta[x_c - x^+ m_{\perp_c} e^{y^*_c}/\sqrt{\hat s}]. \tag{16}$$

Here $d^3\hat\sigma_{gg\to c}/dy^*_c/dk^2_{\perp_c}$ is the differential short distance cross section for c-quark production in the gg-fusion process, for which we use the next-to-leading order (NLO) result from Ref. [27]. $g_p(x,Q)$ is the gluon PDF of the proton, $x^\pm$ are the LC$^\pm$ momentum fractions for the, respectively, projectile and target gluons, and $k_{\perp_c}$ and y^*_c are, correspondingly, the transverse momentum and the rapidity of the produced c-quark in the gluon-gluon c.m. frame. $\hat s = x^+x^- s$ is the c.m. energy squared for the gg scattering, while $s \simeq 2E_p m_p$ is the one for the proton-proton collision, m_p being the proton mass. In the following, unless specified otherwise, we set the factorization $\mu_{\rm F}$ and renormalization $\mu_{\rm R}$ scales equal to c-quark transverse mass $m_{\perp_c} = \sqrt{m_c^2 + k^2_{\perp_c}}$, while using $m_c = 1.3$ GeV for the charm quark mass. In the argument of the δ function in Eq. (16), we neglected the difference between the energy fraction x_c of the c-quark and its LC$^+$ momentum fraction.

In Fig. 1, we plot the CR spectrum-weighted moment for charm production $Z^c_{p\text{-air}}(E,\gamma)$, calculated for $\gamma = 3$, using gluon PDFs from three-flavor NLO PDF sets CT14nlo_NF3 [28], ABMP16_3_nlo [29], and NNPDF31_nlo_pch_as_0118_nf_3 [30], as implemented in the LHAPDF package [31]. For all the gluon PDFs employed, we observe a similar energy dependence of $Z^c_{p\text{-air}}$. A slightly stronger energy rise of the Z factor based

[1]Regarding the prompt neutrino fluxes, nuclear corrections to this approximation have been studied in Ref. [13].

[2]In the following, we approximate the air composition by its most abundant element, nitrogen: $\langle A_{\rm air}\rangle/\sigma^{\rm inel}_{p\text{-air}} \simeq 14/\sigma^{\rm inel}_{pN}$, and use the predictions of the QGSJET-II model [26] for $\sigma^{\rm inel}_{pN}$.

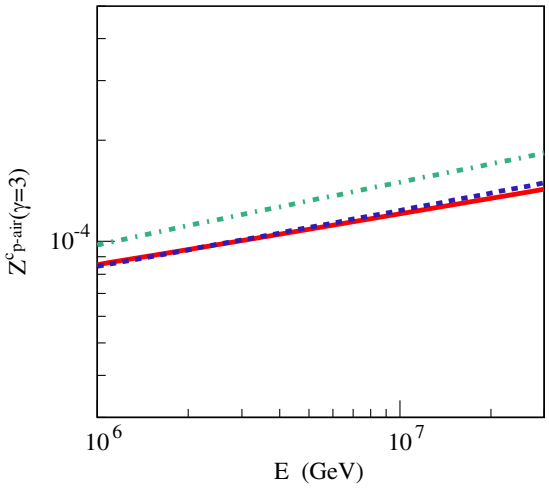

FIG. 1. Energy dependence of the CR spectrum-weighted moment of c-quark production spectrum $Z^c_{p\text{-air}}(E,\gamma)$ for proton-air interactions, calculated using $\gamma = 3$ and employing gluon PDFs from CT14nlo_NF3 (solid), ABMP16_3_nlo (dashed), and NNPDF31_nlo_pch_as_0118_nf_3 (dash-dotted) PDF sets.

on the NNPDF3.1 parametrization is due to a somewhat steeper low-x rise of the respective gluon PDF (see Fig. 2).

In Fig. 3, we illustrate the range of the LC momentum fractions $x^{\pm}$ of the projectile and target gluons, corresponding to maximal contributions to $Z^c_{p\text{-air}}$, for the considered PDF sets. To this end, we plot, for $E = 1$ PeV and $\gamma = 3$, the corresponding distributions $dZ^c_{p\text{-air}}/dx^{\pm}$, as defined by Eq. (15), with $d\sigma^{c(gg)}_{pp}/dx_c$ being replaced by the respective integrands from the rhs of Eq. (16). Clearly, the main contribution to $Z^c_{p\text{-air}}$ comes from relatively high values of $x^+ \sim x_c$, since low x_c is suppressed by the factor $x_c^{\gamma-1}$ [cf. Eqs. (15) and (16)]. On the other hand, the target gluon PDF is mostly probed at very small values of $x^- \sim m_c^2/(x^+ s) \sim m_c/E$, with E being the charm quark energy, as already stressed in previous studies (e.g., [13]). Therefore, the energy rise of $Z^c_{p\text{-air}}(E,\gamma)$ is intimately related to the low-x rise of the gluon PDF $g_p(x^-,\mu_{\rm F})$, as discussed above.

To estimate the impact of uncertainties related to the primary proton spectral slope, we plot in Fig. 4 the energy dependence of the ratio $Z^c_{p\text{-air}}(E,\gamma = 3.3)/Z^c_{p\text{-air}}(E,\gamma = 3)$, for the considered PDF sets. It is easy to see that a change of the slope of the primary spectrum gives rise to a practically energy-independent rescaling of $Z^c_{p\text{-air}}$. This is due to the fact that such a change has a negligible effect on the range of relevant x^- values in Eqs. (15) and (16), while causing an additional suppression of small x^+ values, as illustrated in Fig. 5 for the CT14nlo_NF3 PDF set. It is noteworthy that the obtained dependence of $Z^c_{p\text{-air}}$ on the primary spectrum slope is substantially weaker, compared to the corresponding dependence for prompt neutrino fluxes (see, e.g., [10]), since an additional (and stronger) effect comes in the latter case from the γ dependence of the fragmentation and decay moments,[3] $Z^{\rm fragm}_{c(\bar{c})\to h_c}$ and $Z^{\rm dec}_{h_c\to\nu_\mu}$ [cf. Eqs. (10)–(12)]. Interestingly, Fig. 4 shows that there are only minor differences between the values of the ratio $Z^c_{p\text{-air}}(E,\gamma=3.3)/Z^c_{p\text{-air}}(E,\gamma=3)$ that are obtained for the considered PDF sets; the differences regarding the high-x behavior of the respective gluon PDFs do not make any important impact on the γ dependence of the Z factors for charm production.

Finally, in Fig. 6, we investigate the sensitivity of calculated CR spectrum-weighted moments $Z^c_{p\text{-air}}$ to variations of the factorization $\mu_{\rm F}$ and renormalization $\mu_{\rm R}$ scales: by comparing the respective results obtained with $\mu_{\rm F} = \mu_{\rm R} = m_{\perp_c}$ to the ones calculated using twice larger values for $\mu_{\rm F}$, or for $\mu_{\rm R}$, or for both. Clearly, the sensitivity to higher order pQCD corrections, reflected by the strong dependence of the results on the scale choices, represents the largest uncertainty regarding the perturbative input for calculations of prompt neutrino fluxes, as already stressed in previous studies [32]. It is noteworthy that the uncertainty regarding the low-x extrapolation of the gluon PDF had been greatly reduced by taking into consideration LHCb data on forward charm production [12,33–35].

IV. INTRINSIC CHARM

Let us now discuss the nonperturbative contribution of the so-called intrinsic charm [36,37], which can potentially enhance prompt neutrino fluxes [38]. In some approaches, the corresponding charm production is linked to interactions of constituent charm (anti)quarks from the respective Fock states of the proton (e.g., $|uudc\bar{c}\rangle$) with a target gluon, via the $cg \to cg$ hard scattering process (see, e.g., [39,40]). The picture one has in mind corresponds to a dense gluon cloud originating from the target and incoming on the projectile proton, with some of these gluons hitting the constituent charm (anti)quarks. In such a case, the corresponding contribution to prompt neutrino fluxes is essentially proportional to the gluon PDF of air nuclei, $g_{\rm air}(x^-,Q) \simeq \langle A_{\rm air}\rangle g_p(x^-,Q)$, probed at very small values of the LC$^-$ momentum fraction $x^- \sim m_c^2/(x^+ s)$ and relatively low Q. Consequently, one obtains the same A enhancement of charm production ($\propto\langle A_{\rm air}\rangle$) as for the perturbative generation of charm [cf. Eqs. (15) and (16)] and, more importantly, the same kind of energy rise: $\propto g_p(x^-,Q)|_{x^-\sim m_c^2/(x^+s)}$.

What is missed in the above-discussed approaches is that, at the very high energies we are interested in, the basic valence quark configuration is surrounded by an extensive "coat" formed by gluons and sea quarks and, more importantly, that this coat covers a substantially larger transverse area than the compact valence quark "core" [41]. As a consequence, high-energy proton-proton

[3] See, e.g., Table 3 in Ref. [7].

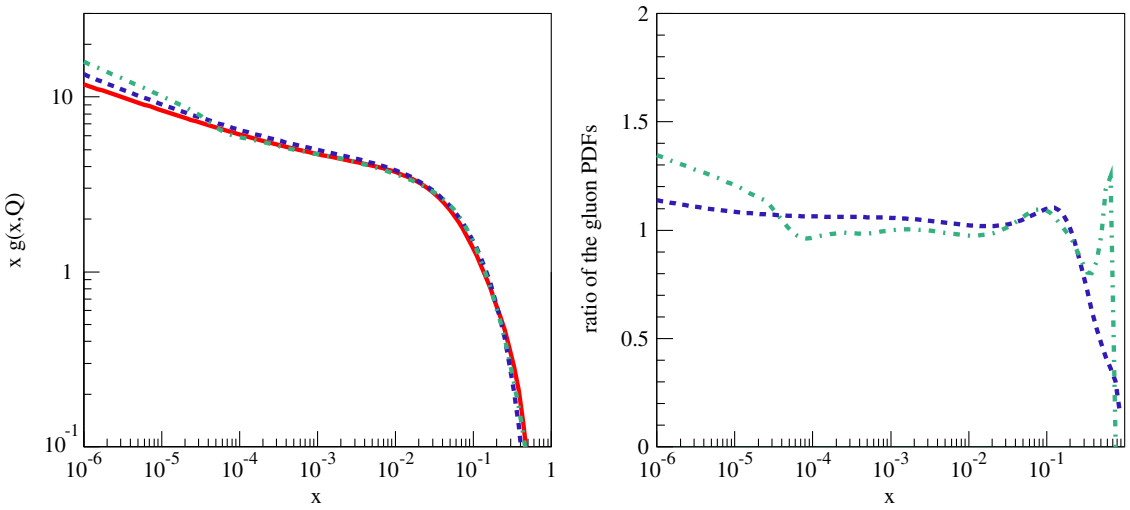

FIG. 2. Left: x dependence of the gluon PDF $g_p(x, Q)$, for $Q = 2$ GeV, for the considered PDF sets; the meaning of the lines is the same as in Fig. 1. Right: the ratios of the gluon PDFs, for $Q = 2$ GeV, from the ABMP16_3_nlo and NNPDF31_nlo_pch_as_0118_nf_3 sets to the one of the CT14nlo_NF3 PDF set—dashed and dash-dotted lines, respectively.

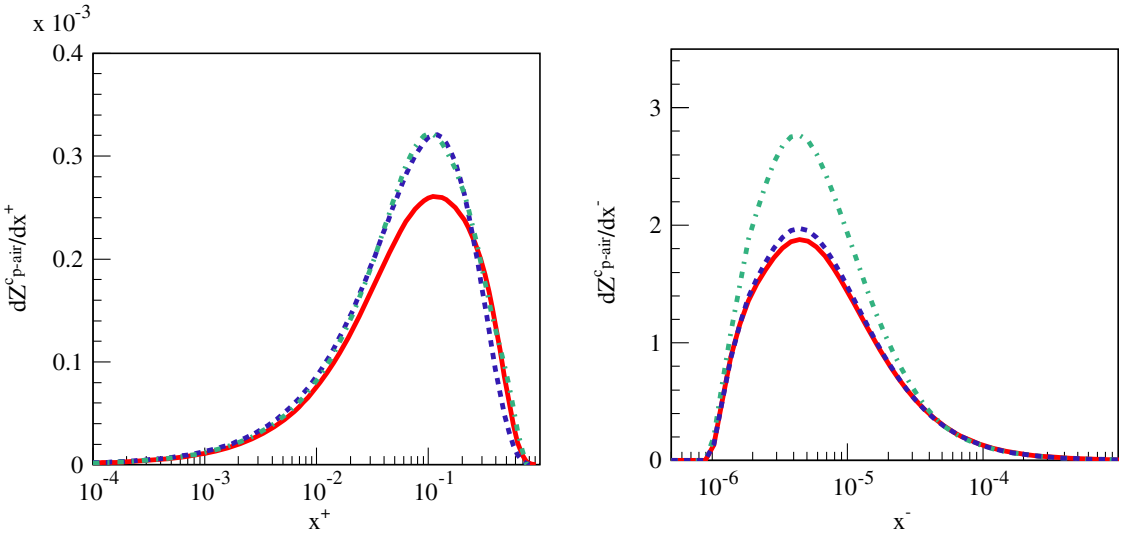

FIG. 3. Distributions of the LC momentum fractions $x^{\pm}$ for, respectively, projectile (left) and target (right) gluons, $dZ^c_{p\text{-air}}/dx^{\pm}$, for $E = 1$ PeV and $\gamma = 3$. The meaning of the lines is the same as in Fig. 1.

(proton-nucleus) collisions are dominated by multiple scattering processes between such nonvalence partons and it is this multiple scattering that unitarizes the respective interaction cross sections.

The above reasoning applies also to the case when the incoming proton is represented by a constituent parton Fock state containing charm (anti)quarks, like $|uudc\bar{c}\rangle$: at sufficiently high energies, these are gluons and sea quarks from the projectile proton, which typically interact with their counterparts from the target. On the other hand, valence quarks usually stay as "spectators" and participate in secondary particle production at the hadronization stage only. Here the crucial point is that an interaction with a nonvalence constituent of the incoming proton is sufficient to destroy the coherence of its original partonic fluctuation and thereby to "free" the charm quark-antiquark pair from its virtual state [42,43].

Thus, at the energies of our interest, interactions of proton Fock states containing intrinsic charm constitute a constant fraction w^c_{intr} of the inelastic cross section,[4] with w^c_{intr} being the overall weight of such states, as suggested already in Ref. [7] (their model 1 for intrinsic charm).

[4]In contrast, in the low-energy limit, the contribution of such states to the inelastic cross section is much suppressed, compared to the basic $|uud\rangle$ configuration. Indeed, since their parton coat remains undeveloped, such states appear to be much more compact than the $|uud\rangle$ state [42].

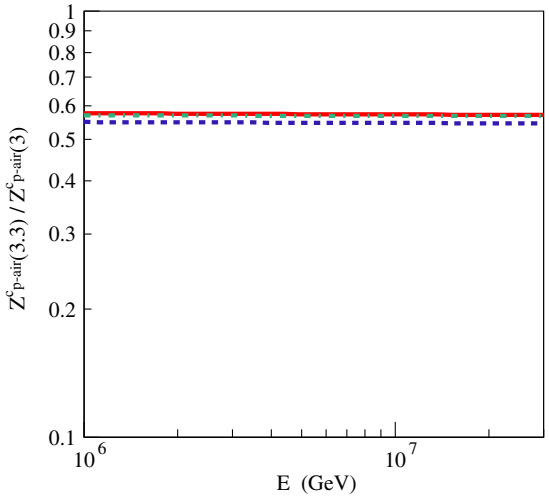

FIG. 4. Energy dependence of the ratio of the CR spectrum-weighted moments $Z^c_{p\text{-air}}(E,\gamma)$, for $\gamma = 3.3$ and $\gamma = 3$. The meaning of the lines is the same as in Fig. 1.

Consequently, the corresponding contribution to charm (anti)quark production can be formally written as

$$\frac{d\sigma^{c(\mathrm{intr})}_{p\text{-air}}(E,x_c)}{dx_c} = w^c_{\mathrm{intr}}\sigma^{\mathrm{inel}}_{p\text{-air}}(E) f^{(\mathrm{intr})}_c(x_c), \tag{17}$$

with $f^{(\mathrm{intr})}_c(x_c)$ being the (normalized to unity) distribution of the constituent c-quark LC momentum fraction in the proton. The corresponding CR spectrum-weighted moment is thus neither energy nor target mass dependent [cf. Eq. (5)],

$$Z^{c(\mathrm{intr})}_{p\text{-air}}(\gamma) = Z^{c(\mathrm{intr})}_{pp}(\gamma) = w^c_{\mathrm{intr}} \int dx_c x_c^{\gamma-1} f^{(\mathrm{intr})}_c(x_c). \tag{18}$$

TABLE I. Calculated CR spectrum-weighted moments $Z^{c(\mathrm{intr})}_{pp}$ for the BHPS and Regge models of intrinsic charm, using different primary spectral slopes.

γ	3	3.3
BHPS model	0.0018	0.0014
Regge model	0.0020	0.0016

For the particular case of $\gamma = 3$, it is thus proportional to the second moment of the constituent c-quark momentum distribution. An important consequence of the energy independence of $Z^{c(\mathrm{intr})}_{p\text{-air}}$ is that the corresponding contribution to the prompt neutrino flux is characterized by the same energy slope as the primary proton flux.

In Table I, we compare the calculated moments $Z^{c(\mathrm{intr})}_{pp}$ for two different distributions $f^{(\mathrm{intr})}_c$ and for the primary proton spectral slopes $\gamma = 3$ and $\gamma = 3.3$. Our first choice corresponds to the original Brodsky-Hoyer-Peterson-Sakai (BHPS) intrinsic charm model [36,37],

$$f^{(\mathrm{intr})}_c(x) \propto x^2\left[\frac{1}{3}(1-x)(1+10x+x^2) + 2x(1+x)\ln x\right]. \tag{19}$$

Alternatively, we consider a Regge ansatz,

$$f^{(\mathrm{intr})}_c(x) \propto x^{-\alpha_\psi}(1-x)^{-\alpha_\psi+2(1-\alpha_N)}. \tag{20}$$

Here the factor $x^{-\alpha_\psi}$ corresponds to the probability to slow down the constituent c quark, with $\alpha_\psi \simeq -2$ being the intercept of the $c\bar{c}$ Regge trajectory [44]. On the other hand, the limit $x \to 1$ is defined by the probability to slow down the remaining ("dressed") valence quark configuration

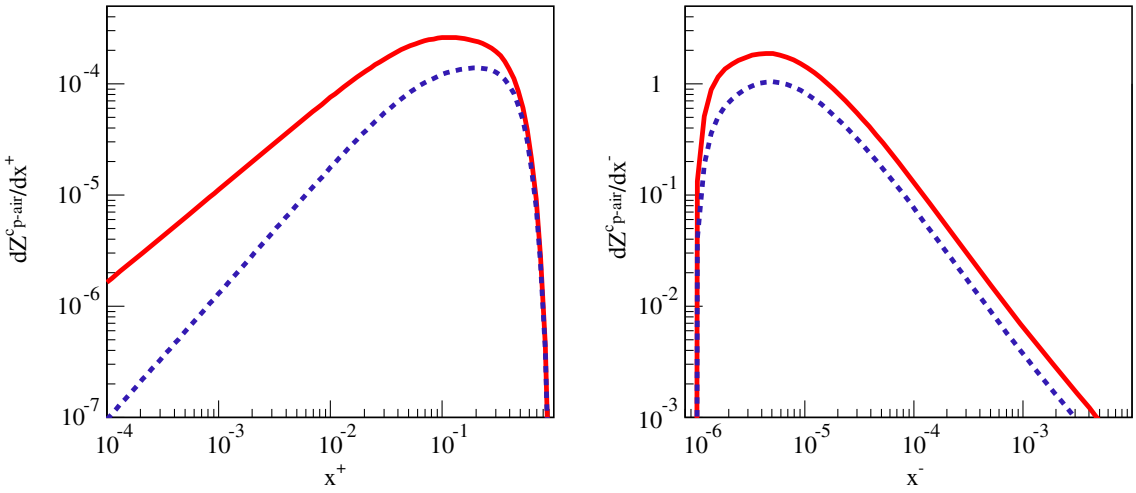

FIG. 5. Distributions of the LC momentum fractions $x^\pm$ for, respectively, projectile (left) and target (right) gluons, $dZ^c_{p\text{-air}}/dx^\pm$, for $E = 1$ PeV, using gluon PDF from the CT14nlo_NF3 set. Solid lines correspond to $\gamma = 3$ and dashed ones to $\gamma = 3.3$.

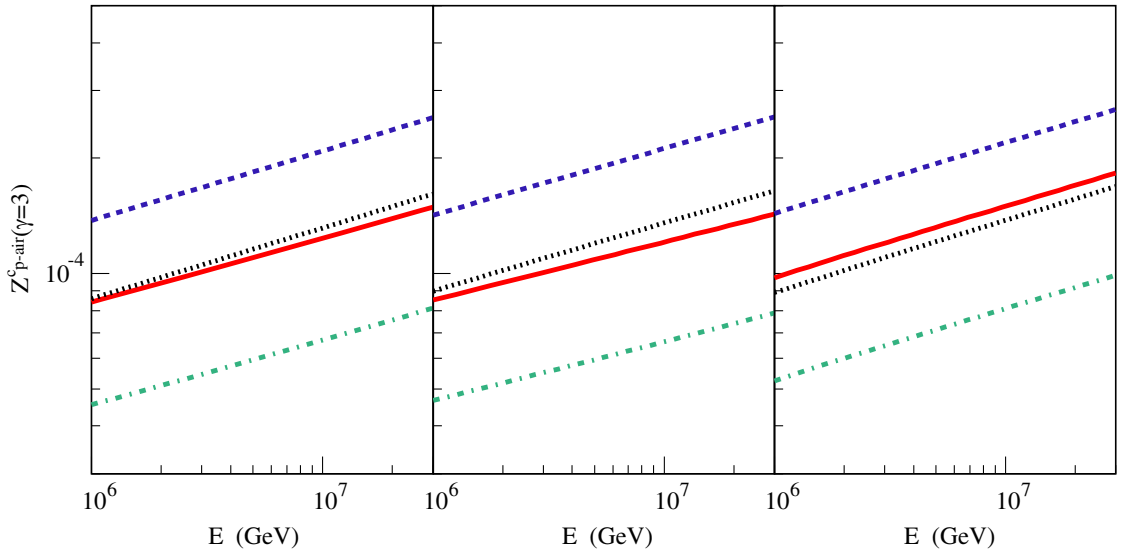

FIG. 6. CR spectrum-weighted moments of c-quark production spectrum $Z^c_{p\text{-air}}(E,\gamma)$, for $\gamma = 3$, calculated using different combinations of the factorization and renormalization scales: $(\mu_F, \mu_R) = (1,1)m_{\perp_c}$ (solid), $(\mu_F, \mu_R) = (2,1)m_{\perp_c}$ (dashed), $(\mu_F, \mu_R) = (1,2)m_{\perp_c}$ (dot-dashed), and $(\mu_F, \mu_R) = (2,2)m_{\perp_c}$ (dotted). The graphs in the left, middle, and right panels are based on gluon PDFs from ABMP16_3_nlo, CT14nlo_NF3, and NNPDF31_nlo_pch_as_0118_nf_3 PDF sets, respectively.

$(uud\bar{c})$, which contributes the factor $(1-x)^{-\alpha_\psi+2(1-\alpha_N)}$, with $\alpha_N \simeq -0.5$ [45].

In both cases, we choose w^c_{intr} such that the total LC momentum fraction of the proton, carried by c and $\bar{c}$, equals 1%, as suggested by the global analyses of the proton PDFs by the CTEQ Collaboration [46],

$$w^c_{\text{intr}} = 0.01/\langle x^{c+\bar{c}}_{uud c\bar{c}}\rangle = 0.01/\left[2\int dx x f^{(\text{intr})}_c(x)\right]. \quad (21)$$

As we can see in Table I, the calculated moments $Z^{c(\text{intr})}_{pp}$ depend weaker on the primary slope γ than $Z^c_{p\text{-air}}$ for perturbative charm production (cf. Fig. 4). This is not surprising since for both our choices for the intrinsic charm model, the distributions $f^{(\text{intr})}_c(x_c)$, shown in Fig. 7, peak at larger values of x_c compared to $dZ^c_{p\text{-air}}/dx^+$ shown in Fig. 3 (left). Further, despite the fact that the fraction of proton LC momentum, carried by charm (anti)quarks, is the same for both our models of intrinsic charm, we obtained somewhat larger $Z^{c(\text{intr})}_{pp}$ when using the Regge ansatz, Eq. (20). This is because that distribution is shifted toward higher x values, compared to the one of the BHPS model, while the CR spectrum-weighted moments are proportional to the second moment of $f^{(\text{intr})}_c$ for $\gamma = 3$ or to an even higher moment for a steeper CR spectrum.

If we formally compared the magnitudes of the Z factors from Table I to the ones corresponding to perturbative charm production, plotted in Fig. 1, we would come to the conclusion that even a subpercent contribution of intrinsic charm would be sufficient to dominate the prompt

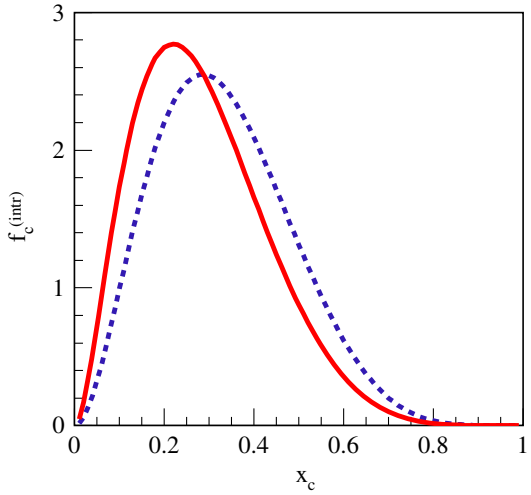

FIG. 7. Distribution of the constituent c-quark LC momentum fraction in the proton, for the BHPS model (solid line) and for the Regge ansatz (dashed line).

atmospheric flux of neutrinos. However, such a comparison may be misleading since the hadronization of constituent charm (anti)quarks can proceed differently, compared to the perturbatively generated ones; hence, our reasoning in Sec. II may be inapplicable to the case of intrinsic charm. Indeed, a constituent c quark is likely to recombine with a valence diquark of the proton to form a charmed baryon (e.g., $c + ud \to \Lambda_c^+$), as suggested by measurements of the Λ_c production asymmetry by the SELEX experiment [47]. In particular, such a picture is implicit in the so-called meson-baryon models of intrinsic charm [48]. Therefore, a

quantitative comparison of the perturbative and nonperturbative contributions to prompt neutrino fluxes can only be performed at the level of neutrino production, taking into consideration the differences between the hadronization mechanisms for the two cases, as was done in previous studies (see, e.g., [38]). Nevertheless, the relatively large values of the Z factors listed in Table I indicate that uncertainties regarding the potential nonperturbative contribution to prompt neutrino fluxes may dominate the ones corresponding to perturbative charm production.

V. CONCLUSIONS

In this work, we addressed the prompt contribution to the atmospheric neutrino flux. Concentrating on the particular case of muonic (anti)neutrinos, we demonstrated that in the energy range of practical interest, the problem can be studied at the level of charm (anti)quark production. Indeed, using the collinear factorization framework of pQCD, we were able to conveniently factorize out both the fragmentation functions for charm (anti)quarks and the decay distributions for charmed hadrons, thereby expressing the prompt flux of atmospheric neutrinos via CR spectrum-weighted moments (Z factors) of production spectra for charm (anti)quarks.

We illustrated the advantages of the method by studying the dependence of our results on the choice of gluon PDFs employed, on the value of the primary CR spectral slope, and on the variations of the factorization and renormalization scales involved in the perturbative evaluation of charm (anti)quark production. We investigated also the range of momentum fractions of both projectile and target gluons, which correspond to maximal contributions to prompt atmospheric neutrino fluxes.

Additionally, we discussed the nonperturbative contribution to the prompt neutrino flux, related to the intrinsic charm content of the proton, using two parametrizations for momentum distributions of constituent charm (anti)quarks in the proton. We demonstrated that the corresponding Z factors take a particularly simple form, being neither energy nor target mass number dependent in the energy range of interest. Consequently, the corresponding contribution to the prompt neutrino flux should be characterized by the same energy slope as the primary CR flux.

However, our approach may be inapplicable for a quantitative comparison of the perturbative and nonperturbative contributions to prompt neutrino fluxes because of potentially different hadronization mechanisms in the two cases. Nevertheless, it is worth stressing that our observation regarding the energy dependence of the contribution of the intrinsic charm to the atmospheric neutrino spectrum, namely, that it is characterized by the same spectral slope as the primary CR spectrum, remains valid, regardless the hadronization mechanism. Since the corresponding perturbative contribution is characterized by a flatter spectral slope [cf. Fig. 1 and Eq. (4)], this offers one a possibility to disentangle the two contributions, based on IceCube data, once a sufficient experimental statistics becomes available at the highest neutrino energies.

ACKNOWLEDGMENTS

S. O. acknowledges enlightening discussions with S. Brodsky and a financial support from Deutsche Forschungsgemeinschaft (Project No. 465275045). M. V. G. is grateful to M. Benzke for useful cross-checks and to M. H. Reno for discussions and clarifications on her works on related topics. The work of M. V. G. was partially supported by the Bundesministerium für Bildung und Forschung, under Contract No. 05H21GUCCA. G. S. acknowledges support by the Bundesministerium für Bildung und Forschung, under Grants No. 05A17GU1 and No. 05A20GU2.

[1] M. G. Aartsen *et al.* (IceCube Collaboration), First Observation of PeV Neutrinos with IceCube, Phys. Rev. Lett. **111**, 021103 (2013).
[2] M. G. Aartsen *et al.* (IceCube Collaboration), Evidence for high-energy extraterrestrial neutrinos at the IceCube detector, Science **342**, 1242856 (2013).
[3] T. K. Gaisser, *Cosmic Rays and Particle Physics* (Cambridge University Press, Cambridge, England 1990).
[4] P. Lipari, Lepton spectra in the Earth's atmosphere, Astropart. Phys. **1**, 195 (1993).
[5] G. D. Barr, T. K. Gaisser, P. Lipari, S. Robbins, and T. Stanev, A three-dimensional calculation of atmospheric neutrinos, Phys. Rev. D **70**, 023006 (2004).
[6] M. Honda, T. Kajita, K. Kasahara, S. Midorikawa, and T. Sanuki, Calculation of atmospheric neutrino flux using the interaction model calibrated with atmospheric muon data, Phys. Rev. D **75**, 043006 (2007).
[7] M. Thunman, G. Ingelman, and P. Gondolo, Charm production and high energy atmospheric muon and neutrino fluxes, Astropart. Phys. **5**, 309 (1996).
[8] L. Pasquali, M. H. Reno, and I. Sarcevic, Lepton fluxes from atmospheric charm, Phys. Rev. D **59**, 034020 (1999).
[9] R. Enberg, M. H. Reno, and I. Sarcevic, Prompt neutrino fluxes from atmospheric charm, Phys. Rev. D **78**, 043005 (2008).
[10] A. Bhattacharya, R. Enberg, M. H. Reno, I. Sarcevic, and A. Stasto, Perturbative charm production and the prompt

atmospheric neutrino flux in light of RHIC and LHC, J. High Energy Phys. 06 (2015) 110.
[11] M. V. Garzelli, S. Moch, and G. Sigl, Lepton fluxes from atmospheric charm revisited, J. High Energy Phys. 10 (2015) 115.
[12] R. Gauld, J. Rojo, L. Rottoli, and J. Talbert, Charm production in the forward region: Constraints on the small-x gluon and backgrounds for neutrino astronomy, J. High Energy Phys. 11 (2015) 009.
[13] A. Bhattacharya, R. Enberg, M. H. Reno, I. Sarcevic, and A. Stasto, Prompt atmospheric neutrino fluxes: Perturbative QCD models and nuclear effects, J. High Energy Phys. 11 (2016) 167.
[14] M. Benzke, M. V. Garzelli, B. Kniehl, G. Kramer, S. Moch, and G. Sigl, Prompt neutrinos from atmospheric charm in the general-mass variable-flavor-number scheme, J. High Energy Phys. 12 (2017) 021.
[15] G. Kulikov and G. Khristiansen, On the size spectrum of extensive air showers, Sov. Phys. JETP **8**, 441 (1959).
[16] W. D. Apel *et al.* (KASCADE-Grande Collaboration), Ankle-like feature in the energy spectrum of light elements of cosmic rays observed with KASCADE-Grande, Phys. Rev. D **87**, 081101 (2013).
[17] T. Antoni *et al.* (KASCADE Collaboration), KASCADE measurements of energy spectra for elemental groups of cosmic rays: Results and open problems, Astropart. Phys. **24**, 1 (2005).
[18] W. D. Apel *et al.* (KASCADE-Grande Collaboration), KASCADE-Grande measurements of energy spectra for elemental groups of cosmic rays, Astropart. Phys. **47**, 54 (2013).
[19] W. D. Apel *et al.* (KASCADE-Grande Collaboration), Knee-Like Structure in the Spectrum of the Heavy Component of Cosmic Rays Observed with KASCADE-Grande, Phys. Rev. Lett. **107**, 171104 (2011).
[20] M. G. Aartsen *et al.* (IceCube Collaboration), Cosmic ray spectrum and composition from PeV to EeV using 3 years of data from IceTop and IceCube, Phys. Rev. D **100**, 082002 (2019).
[21] M. Kachelrieß and S. Ostapchenko, Neutrino yield from Galactic cosmic rays, Phys. Rev. D **90**, 083002 (2014).
[22] K.-H. Kampert and M. Unger, Measurements of the cosmic ray composition with air shower experiments, Astropart. Phys. **35**, 660 (2012).
[23] P. Abreu *et al.* (Pierre Auger Collaboration), The energy spectrum of cosmic rays beyond the turn-down around 10^{17} eV as measured with the surface detector of the Pierre Auger Observatory, Eur. Phys. J. C **81**, 966 (2021).
[24] J. Engel, T. K. Gaisser, T. Stanev, and P. Lipari, Nucleus-nucleus collisions and interpretation of cosmic ray cascades, Phys. Rev. D **46**, 5013 (1992).
[25] M. Glück, E. Reya, and M. Stratmann, Heavy quarks at high energy colliders, Nucl. Phys. **B422**, 37 (1994).
[26] S. Ostapchenko, Monte Carlo treatment of hadronic interactions in enhanced Pomeron scheme: QGSJET-II model, Phys. Rev. D **83**, 014018 (2011).
[27] P. Nason, S. Dawson, and R. K. Ellis, The one particle inclusive differential cross section for heavy quark production in hadronic collisions, Nucl. Phys. **B327**, 49 (1989).
[28] S. Dulat, T.-J. Hou, J. Gao, M. Guzzi, J. Huston, P. Nadolsky, J. Pumplin, C. Schmidt, D. Stump, and C.-P. Yuan, New parton distribution functions from a global analysis of quantum chromodynamics, Phys. Rev. D **93**, 033006 (2016).
[29] S. Alekhin, J. Blümlein, and S. Moch, NLO PDFs from the ABMP16 fit, Eur. Phys. J. C **78**, 477 (2018).
[30] R. D. Ball, V. Bertone, F. Cerutti, S. Carrazza, L. Del Debbio, S. Forte, P. Groth-Merrild, A. Guffanti, N. P. Hartland, Z. Kassabov *et al.* (NNPDF Collaboration), Parton distributions from high-precision collider data, Eur. Phys. J. C **77**, 663 (2017).
[31] A. Buckley, J. Ferrando, S. Lloyd, K. Nordström, B. Page, M. Rüfenacht, M. Schönherr, and G. Watt, LHAPDF6: Parton density access in the LHC precision era, Eur. Phys. J. C **75**, 132 (2015).
[32] O. Zenaiev, M. V. Garzelli, K. Lipka, S.-O. Moch, A. Cooper-Sarkar, F. Olness, A. Geiser, and G. Sigl (PROSA Collaboration), Improved constraints on parton distributions using LHCb, ALICE and HERA heavy-flavour measurements and implications for the predictions for prompt atmospheric-neutrino fluxes, J. High Energy Phys. 04 (2020) 118.
[33] R. Gauld and J. Rojo, Precision Determination of the Small-x Gluon from Charm Production at LHCb, Phys. Rev. Lett. **118**, 072001 (2017).
[34] O. Zenaiev *et al.* (PROSA Collaboration), Impact of heavy-flavour production cross sections measured by the LHCb experiment on parton distribution functions at low x, Eur. Phys. J. C **75**, 396 (2015).
[35] M. V. Garzelli, S. Moch, O. Zenaiev, A. Cooper-Sarkar, A. Geiser, K. Lipka, R. Placakyte, and G. Sigl (PROSA Collaboration), Prompt neutrino fluxes in the atmosphere with PROSA parton distribution functions, J. High Energy Phys. 05 (2017) 004.
[36] S. J. Brodsky, P. Hoyer, C. Peterson, and N. Sakai, The intrinsic charm of the proton, Phys. Lett. **93B**, 451 (1980).
[37] S. J. Brodsky, C. Peterson, and N. Sakai, Intrinsic heavy-quark states, Phys. Rev. D **23**, 2745 (1981).
[38] R. Laha and S. J. Brodsky, IceCube can constrain the intrinsic charm of the proton, Phys. Rev. D **96**, 123002 (2017).
[39] A. V. Giannini, V. P. Goncalves, and F. S. Navarra, Intrinsic charm contribution to the prompt atmospheric neutrino flux, Phys. Rev. D **98**, 014012 (2018).
[40] R. Maciuła and A. Szczurek, Intrinsic charm in the nucleon and charm production at large rapidities in collinear, hybrid and k_T-factorization approaches, J. High Energy Phys. 10 (2020) 135.
[41] L. Frankfurt, M. Strikman, and C. Weiss, Dijet production as a centrality trigger for pp collisions at CERN LHC, Phys. Rev. D **69**, 114010 (2004).
[42] S. J. Brodsky and P. Hoyer, Nucleus as a Color Filter in QCD: Hadron Production in Nuclei, Phys. Rev. Lett. **63**, 1566 (1989).
[43] S. J. Brodsky, P. Hoyer, A. H. Mueller, and W.-K. Tang, New QCD production mechanisms for hard processes at large x, Nucl. Phys. **B369**, 519 (1992).
[44] A. B. Kaidalov, $J/\psi\, c\bar{c}$ production in e^+e^- and hadronic interactions, JETP Lett. **77**, 349 (2003).

[45] A. B. Kaidalov and O. I. Piskunova, Inclusive spectra of baryons in the quark-gluon string model, Z. Phys. C **30**, 145 (1986).

[46] S. Dulat, T.-J. Hou, J. Gao, J. Huston, J. Pumplin, C. Schmidt, D. Stump, and C.-P. Yuan, Intrinsic charm parton distribution functions from CTEQ-TEA global analysis, Phys. Rev. D **89**, 073004 (2014).

[47] F. G. Garcia *et al.* (SELEX Collaboration), Hadronic production of Λ_c from 600 GeV/c π^-, Σ^- and p beams, Phys. Lett. B **528**, 49 (2002).

[48] T. J. Hobbs, J. T. Londergan, and W. Melnitchouk, Phenomenology of nonperturbative charm in the nucleon, Phys. Rev. D **89**, 074008 (2014).